New Insight into Erythrocyte through In Vivo Surface-Enhanced Raman Spectroscopy

Nadezda A. Brazhe,[†*] Salim Abdali,[‡] Alexey R. Brazhe,[†] Oksana G. Luneva,[†] Nadezda Y. Bryzgalova,[†] Eugenia Y. Parshina,[†] Olga V. Sosnovtseva,[§] and Georgy V. Maksimov[†]

[†]Biophysics Department, Biological Faculty, Moscow State University, Moscow, Russian Federation; [‡]Danish Cancer Society, Copenhagen, Denmark and Department of Medical Engineering, Technical University of Denmark, Denmark; and [§]Department of Biomedical Sciences, Copenhagen University, Copenhagen, Denmark

ABSTRACT The article presents a noninvasive approach to the study of erythrocyte properties by means of a comparative analysis of signals obtained by surface-enhanced Raman spectroscopy (SERS) and resonance Raman spectroscopy (RS). We report step-by-step the procedure for preparing experimental samples containing erythrocytes in their normal physiological environment in a mixture of colloid solution with silver nanoparticles and the procedure for the optimization of SERS conditions to achieve high signal enhancement without affecting the properties of living erythrocytes. By means of three independent techniques, we demonstrate that under the proposed conditions a colloid solution of silver nanoparticles does not affect the properties of erythrocytes. For the first time to our knowledge, we describe how to use the SERS-RS approach to study two populations of hemoglobin molecules inside an intact living erythrocyte: submembrane and cytosolic hemoglobin (Hb_{sm} and Hb_c). We show that the conformation of Hb_{sm} differs from the conformation of Hb_c. This finding has an important application, as the comparative study of Hb_{sm} and Hb_c could be successfully used in biomedical research and diagnostic tests.

INTRODUCTION

Conformations and properties of molecules in different compartments of living cells merit attention, for it has become clear that purified molecules in a test tube behave differently when compared to those in their natural cellular environment. To this end, live-cell studies with Raman spectroscopy (RS) have recently attracted great interest, because RS provides information about the structure of biomolecules in vivo with no effect on the cell's integrity (1–3). RS requires a relatively high concentration of molecules, usually $>10^{-4}$–10^{-3}M, and therefore high numbers of cells. Surface-enhanced RS (SERS) is another Raman tool, which utilizes the effect of plasmon resonance and charge transfer when a molecule is found in the vicinity of a nanoparticle (NP) or a nanostructured surface, usually silver (Ag) or gold (Au) (4,5). Due to plasmon resonance and charge transfer, the cross section of Raman scattering and therefore the intensity of the Raman signal are both greatly enhanced. This has made possible studies of molecules at concentrations $<<10^{-6}$M and so-called single-molecule studies (6). NP plasmon resonance occurs only when the distance between the NP surface and the studied molecule is relatively small. It reaches the highest intensity at optimal distances at ~15–20 nm from the NP surface and decreases significantly for greater distances (5,7–9). The challenging aspect of this is to use SERS to study single molecules inside an individual living cell or in a very diluted cell sample. However, despite the numerous advantages of SERS, large biomolecules and living cells are still difficult to study using this method, and only a few results have been reported on SERS of proteins and cells (10–13). The possible invasivity of NPs for living cells is another complication in SERS studies. So far, there are no reports on NP effect on living cells or on optimization of SERS conditions to maintain cells in an unaffected live state while, at the same time, achieving the highest possible enhancement.

Erythrocytes are widely used objects in biomedical research and in diagnostic tests (14). Since many drugs are injected directly into the blood stream, it is important to have methods for analyzing drug effects on various hemoglobin subpopulations and on erythrocytes as such.

All hemoglobin molecules in erythrocytes can be divided into two groups: free cytosolic Hb and submembrane hemoglobin that interacts with plasma membrane. There are two possible sites of interaction of Hb_{sm} with plasma membrane: the cytosolic part of an anion exchanger AE1 (band 3) and membrane lipids (Fig. 1) (15–17). Interaction of Hb with AE1 exchanger is quite well studied in an in vitro system of purified Hb and erythrocyte membrane or purified Hb and cytosolic part of AE1 protein (15–17). That interaction of Hb with membrane lipids is possible, and could be artificially observed (18) seems to be insignificant for living erythrocytes, as lipids are normally masked by membrane proteins or cytoskeleton (19,20). Therefore, the dominating part of submembrane Hb is bound to AE1 exchanger. Cytosolic domain of AE1 exchanger also interacts with spectrin and ankirin, which, together with band 4.1, actin, tropomyosin, and tropomodulin bound on the transmembrane protein glycophorin, form submembrane cytoskeleton (21–23) (Fig. 1). A widespread method for the study of erythrocytes and isolated Hb is absorption spectroscopy (AS) (16,24–28).

Submitted April 6, 2009, and accepted for publication September 15, 2009.

*Correspondence: una@biophys.msu.ru

Editor: Feng Gai.

0006-3495/09/12/3206/9 $2.00

doi: 10.1016/j.bpj.2009.09.029

Despite its virtues (simplicity in handling and in data analysis), AS does not provide any detailed information about Hb structure. In addition, due to the significant difference in concentrations of Hb_{sm} and Hb_c ($Hb_{sm} \leq 0.5\%$ Hb_c) (15), it is impossible to study the properties of Hb_{sm} in an intact erythrocyte with AS. However, such a difference in concentrations does allow us to study Hb_c molecules in erythrocytes by means of RS or resonance RS, because the contribution from Hb_{sm} to the RS spectrum is negligible. To investigate Hb_{sm} molecules, we suggest the use of SERS. Adding NPs to a highly diluted blood sample yields an enhancement of Raman scattering only from those Hb molecules that interact with the plasma membrane (located at $\approx$15–20 nm from the outer membrane surface)—i.e., from Hb_{sm} (Fig. 1). As cytoskeleton and submembrane proteins obstructs Hb from approaching lipids of plasma membrane, the amount of free cytosolic Hb_c under membrane can be significantly less than the amount of Hb bound to AE1 protein. We could therefore expect Hb_c not to contribute essentially to SERS spectra of erythrocytes.

In this article, we demonstrate a new approach of a comparative SERS and RS study of living erythrocytes, with emphasis on the optimization of the SERS conditions necessary to achieve the highest possible signal enhancement without affecting the cell properties. We propose to use this approach to study two subpopulations of hemoglobin molecules: submembrane hemoglobin (Hb_{sm}) and cytosolic hemoglobin (Hb_c) inside intact living erythrocytes, and we show how to distinguish one subpopulation from the other.

MATERIALS AND METHODS

Preparation of Ag NP colloid, experimental samples of erythrocytes, hemoglobin, and erythrocyte ghosts, and the optimization of SERS conditions

Ag NP colloid solution was prepared by the reduction of $AgNO_3$ with hydroxylamine hydrochloride in NaOH solution, described as variant C by Leopold and Lendl (29). The reaction between $AgNO_3$ and hydroxylamine hydrochloride resulted in the formation of Ag NPs in the solution (containing Na^+, Cl^-, and NO_3^- ions in mM concentration), nitrogen oxides, and N_2, which evaporate during the NPs maturation. In SERS experiments we used erythrocyte samples prepared from whole blood taken from male Wistar rats and diluted 10^4 times with the appropriate physiological buffers (Alen saline or Tris-based saline). Considering the low concentration of ions in Ag NP solution, it was necessary to compensate for the low osmolarity in the mixture of the Ag NP solution and the erythrocyte sample. We therefore used two successive dilutions of blood: 1), 100-times dilution of blood with normal physiological saline (first dilution results in sample 1); and 2), 100-times dilution of sample 1 with hyperosmolar physiological saline (second dilution results in sample 2). The hyperosmolar physiological saline was prepared by increasing the concentrations of all normal physiological saline components to obtain an experimental sample with a normal concentration of ions after mixing sample 2 with Ag NP solution. Sample 2 was mixed with Ag NP solution in a certain volume ratio immediately after the preparation of the sample 2, so erythrocytes were exposed to hyperosmolar conditions for no more than 10 s. The sample 2 and Ag NPs mixing resulted in experimental erythrocyte sample (EES) with normal osmolarity

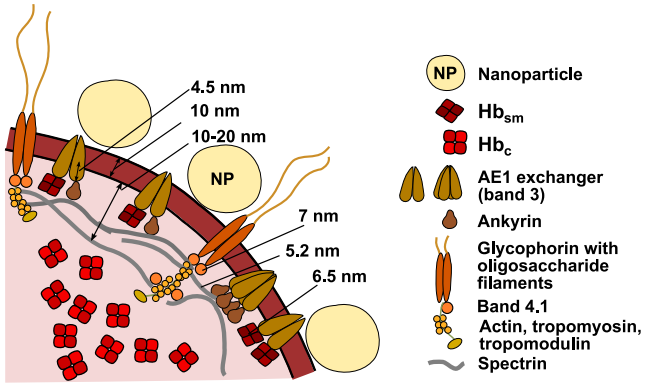

FIGURE 1 Schematic drawing of an erythrocyte in the submembrane region with transmembrane proteins, cytoskeleton, submembrane hemoglobin (Hb_{sm}) bound to the AE1 exchanger, cytosolic hemoglobin (Hb_c), and Ag nanoparticles next to the cell membrane. Distances between the plasma membrane and the cytoskeleton and the size of proteins are taken from the literature (22,24,25).

for erythrocytes. The composition of both normal and hyperosmolar Tris-based and Alen saline, and details of their preparation, are available in the Supporting Material.

A SERS spectrum was recorded directly after the preparation of EES and was the result of 10 accumulations recorded for 10 s each.

SERS and RS spectra were obtained using a ChiralRaman setup (BioTools, Jupiter, FL) with a 532-nm laser. Considering the absorbance of Hb at this wavelength, we had resonance SERS and resonance RS. It is important to note that, due to this resonance condition, we selectively probed heme in Hb molecules in an intact erythrocyte and the possible input of scattering from transmembrane proteins or cytoskeleton is negligible.

Previously, we had found that varying the Ag NP content in the sample had a great influence on the SERS spectra of myoglobin (12). In our experiments, pronounced and clear SERS spectra of erythrocytes were observed when an iterative optimization of the volume ratio of Ag NP solution to the EES was carried out, with the best results coming from [Ag NP solution]:[EES] = 2:3 ratio (see Fig. S1 in the Supporting Material). A further increase in the volume fraction of Ag NPs in the experimental sample yielded only a slight enhancement of the SERS signal, which we found to be unnecessary, so a limitation of the effect of higher Ag NP concentration in the sample could be avoided. We should note that varying the volume ratio of Ag NP solution does not affect peak-shape or relative peak intensities (Fig. S1). Moreover, independent experiments with fixed amount of Ag NPs showed that SERS spectra of erythrocytes taken from different blood samples were similar (Fig. S2). This is evidence of high stability of used Ag NP colloids and signal enhancement. We also observed that SERS spectra of the same erythrocyte sample recorded at 0, 15, and 45 min are identical to each other (Fig. S3). This is evidence of 1), the temporal stability of the signal enhancement; 2), temporal stability of erythrocyte-Ag NP complex; and 3), absence of the erythrocyte photodamage by laser light. In addition, we found that the SERS spectra of erythrocytes did not depend on the type of physiological saline used for blood dilution. This indicates the stability of Ag NPs in both Alen and Tris-based salines.

For RS measurements, we used blood diluted 100 times by normal physiological saline (Alen or Tris-based salines). An RS spectrum is the result of 10 accumulations recorded for 10 s each. As in SERS measurements, the Raman spectra of erythrocytes were similar for both salines. In all following SERS and RS experiments, we used Tris-based salines.

To compare SERS and RS spectra of erythrocytes and cytosolic Hb, we isolated Hb from the cytoplasm of erythrocytes from the same blood sample used for the SERS and RS erythrocyte studies. The isolation of Hb was done in a phosphate buffer with low osmolarity, pH 7.2 (see Supporting Material). Hemolysis evoked disruption of the erythrocytic plasma membrane and

leakage of cytosolic Hb_c into the buffer. Centrifugation (4500 × *g*, 10 min) was used to separate the supernatant with isolated cytosolic hemoglobin from the ghosts of erythrocytes containing Hb_{sm} and the remains of Hb_c. For RS measurements, we used supernatant that had been diluted four times, and for SERS measurements, supernatant diluted 200 times.

To illustrate the similarity of SERS spectra of erythrocytes and membrane-bound Hb, we made ghosts of erythrocytes with Hb bound to the AE1 exchanger of the ghost membrane (Hb_{AE1}). Erythrocyte ghosts are closed vesicles that consist of erythrocytic plasma membrane with submembrane cytoskeleton and transmembrane proteins, and do not contain unbound cytosolic Hb. Preparation of erythrocyte ghosts with membrane-bound Hb_{AE1} was done as described in Salhany et al. (30) using ice-cold phosphate buffer (pH 7.4; for details, see Supporting Material). For SERS measurements, samples with erythrocyte ghosts were diluted 1000 times. Volume ratio of solution with erythrocyte ghosts or isolated Hb to Ag NPs was as in SERS experiments with erythrocytes: [Ag NP solution]:[erythrocyte ghosts or isolated Hb] = 2:3. Taking into account resonance Raman conditions (due to the wavelength of the laser light), we can be sure that SERS spectrum of erythrocyte ghosts results from vibrations of the heme bonds in Hb_{AE1}.

Methods used for the study of the effect of Ag NP on erythrocytes

Estimation of erythrocyte hemolysis was done by absorption spectroscopy. Resistance of erythrocytes toward hemolysis is a marker of the stability of the plasma membrane and, therefore, is a proper parameter for the study of the effect of exogenous factors on erythrocytes. The procedure for the preparation of the erythrocyte suspension with 10^7 cells/μL was the same as in experiments with preparation of erythrocyte ghosts. Ninety microliters of adjusted erythrocyte suspension was diluted with 810 μL of hyperosmolar Tris-based saline and then mixed with Ag NP solution in the volume ratio [Ag NP solution]:[erythrocyte sample] = 2:3. After this procedure, we obtained an experimental erythrocyte sample with Ag NPs of normal osmolarity. This sample was incubated for 10 min at room temperature and centrifugated (1500 rot/min, 10 min). Supernatant was used for the registration of absorbance spectra (performed with a model No. 556 spectrometer; Hitachi, Tokyo, Japan).

We also prepared two control samples. The first control sample (hereafter referred to as the ''control sample 1'') was prepared in the same way as the erythrocyte sample, except for adding 3 mM of NaCl solution instead of Ag NP solution (the osmolarity of 3 mM NaCl solution is close to that of Ag NP solution). The second control sample (hereafter referred to as the control sample 2) was prepared by the dilution of 90 μL of the erythrocyte suspension with 810 μL of normal Tris-based saline and then mixed with normal Tris-based saline in the same ratio, 3:2, as erythrocyte samples were mixed with Ag NP solution or NaCl. The comparison of erythrocytes-Ag NPs sample with NaCl sample shows the effect of Ag NPs on erythrocyte properties, and the comparison of the NaCl sample and the control sample shows the effect of hyperosmolar saline on erythrocytes. The optical density of a supernatant was estimated at a wavelength of 540 nm. The concentration of Hb in the supernatant was calculated according to the Beer-Lambert law. The percentage of hemolysed erythrocytes was calculated from the number of erythrocytes in the erythrocyte suspension, the concentration of Hb released from the hemolysed erythrocytes, the mean concentration of Hb in rat erythrocytes (5×10^{-3} M), and the mean erythrocyte volume (50 fL).

Estimation of the fluidity of the plasma membrane of erythrocytes was done by electron paramagnetic resonance spectroscopy (EPR). As a probe, we employed a spin-labeled stearic acid analog 16-doxylstearic acid (16-DS; Sigma, St. Louis, MO). It is known that the nitroxyl radical of 16-DS locates at 2.2 nm from the surface of plasma membrane (31). The procedure for the preparation of the erythrocyte suspension with 10^7 cells/μL was as in previous experiments. A quantity of 0.8 mL of erythrocyte suspension was diluted with 1.2 mL of hyperosmolar Tris-based saline and then mixed with 0.8 mL of Ag NP solution. The obtained erythrocyte-Ag NPs sample was centrifugated (1500 rot/min, 10 min at room temperature). We removed 2 mL of supernatant and subsequently added 1.2 mL of hyperosmolar Tris-based saline and 0.8 mL of Ag NP solution. After the second centrifugation, 2 mL of supernatant were removed and the number of erythrocytes was counted in the Gorjaev chamber; it was equal to 10^7 cells/μL. Control samples were prepared in a similar way, except for adding 0.8 mL of 3 mM NaCl solution instead of Ag NPs solution. The 16-DS probe was dissolved in ethanol at a concentration of 25 mM and added to the sample with erythrocytes and Ag NPs with a final concentration of 0.1 mM. After 2 min of extensive shaking, the sample was sucked into glass capillaries. EPR spectra were registered at room temperature on a model No. RE-1308 EPR spectrometer (Radiopan, Smolensk, Russia) with a constant magnetic field, microwave power, and time constant of 3338 Gs, 22 mW, and 0.1 s, respectively. Each measurement was performed in triplicate, and each was the result of seven accumulations. From the parameters of EPR spectra of an 16-DS probe incorporated into the plasma membrane of erythrocytes, we calculated the rotation correlation time τ, as an estimation of membrane fluidity (32). The decrease in τ corresponds to the increase in the membrane fluidity and vice versa.

The morphology of erythrocytes was monitored by optical microscopy using cell fixation in glutaraldehyde according to Gedde et al. (33) with modification. Erythrocyte morphology is an important complex characteristic, dependent upon the physico-chemical and mechanical properties of plasma membrane, and the distribution of membrane lipids, ion fluxes, membrane surface charges, submembrane cytoskeleton, intracellular pH, etc. (34,35), and, therefore, is an important integral parameter in many studies (14,36,37). Two microliters of blood was mixed with 600 μL of hyperosmolar Tris-based saline and then mixed with 400 μL of Ag NP solution (experimental sample) or 3 mM NaCl solution (control sample 1). The control sample 2 was prepared as a dilution of 2 μL of blood with 1000 μL of normal Tris-based saline. After 10-min incubation of obtained samples, 20 μL of 25% glutaraldehyde was added to samples (the final concentration of glutaraldehyde was 1%). After 1 h of incubation, samples were centrifugated (1750 × *g*, 10 min at room temperature) and supernatant was replaced with an equal volume of distilled water. The procedure was repeated four times. For the morphology analysis, a drop of a final sample was placed on the object plate and dried at room temperature. For each sample, three object plates were prepared. Using an Axioplan 2.0 microscope (Carl Zeiss, Oberkochen, Germany), we made light-field photographs of the erythrocytes and then calculated the number of erythrocytes taking the form of a discocyte, an echinocyte, and a stomatocyte. The percentage of each form was estimated as a ratio of the number of cells in this specific form to the total number of counted erythrocytes. Details of erythrocyte morphology and its significance in the determination of erythrocyte viability are discussed in more detail in the Supporting Material.

RESULTS AND DISCUSSION

Spectral analysis

It is well established that almost all peaks in Raman spectra of erythrocytes correspond to the bond vibrations in the heme of all hemoglobin molecules (Fig. 2). Bond vibrations depend on the conformation of heme, which is affected by the ligand (O_2, CO, or NO), the position of the Fe^{2+} ion with respect to the heme ring, and the conformation of the globin (2,38–40). The assignment of the major peaks is shown in Table 1. For the comparison of different spectra, and to have SERS spectra independent of the exact Hb amount in the studied samples, we have normalized the spectra to the sum of intensities in the region of 1618–1503 cm^{-1}. This region originates from certain vibrations of heme bonds in all of the Hb molecules in the sample and is therefore proportional to the total amount of Hb. Fig. 3 *a* shows a normalized SERS spectrum of erythrocytes mixed with Ag NP solution in the

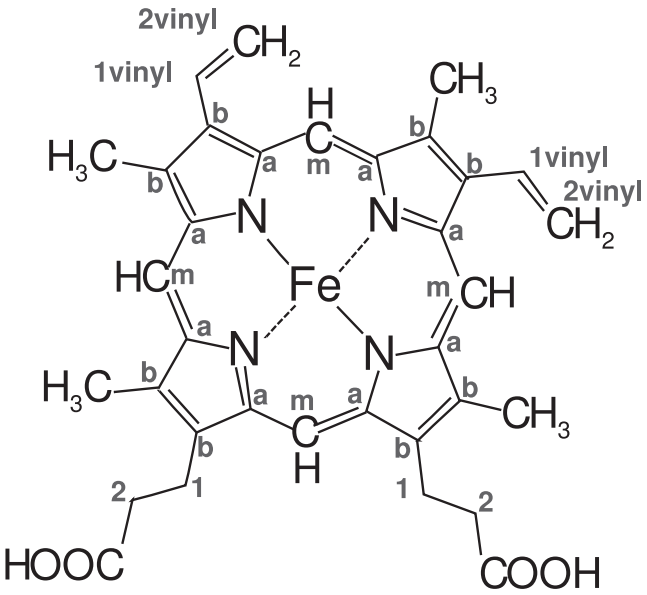

FIGURE 2 Heme molecule with numbered C atoms.

optimized volume ratio [Ag NP solution]:[EES] = 2:3. High blood dilution, used in SERS experiments, produces full oxygenation of Hb molecules in erythrocytes, and this, indeed, is confirmed by all the pronounced peaks in the SERS spectra, which are attributed to oxyhemoglobin (Hb-O_2). The RS spectrum of erythrocytes (prepared from the same blood as for SERS experiments) also consists of peaks attributable to Hb-O_2 (Fig. 3 *b*).

A comparative analysis of SERS and RS spectra from the erythrocytes shows that most of their peaks have the same maximum position. However, the SERS spectrum appears to be much more detailed with higher intensities in the low-frequency range, which is almost unpronounced in the RS spectrum. The absence of complete similarity between SERS and RS spectra of the same molecule is well known and is explained by the NP-evoked enhancement of vibrational transitions that are weak or even unpronounced in RS (5). This SERS peculiarity makes the direct comparison of SERS and RS spectra of erythrocytes quite problematic. However, in the last section of the article, we discuss how the combination of RS and SERS can be used to distinguish between cytosolic and submembrane hemoglobins.

The effect of nanoparticles on erythrocyte properties

We found that erythrocytes, when mixed with Ag NPs, showed higher resistance to hemolysis compared to erythrocytes exposed to dilution in hyperosmolar Tris-based saline and then mixed with NaCl solution, and to erythrocytes in the control sample 2 (Fig. 4 *a*). This result indicates that there is no Ag NP-evoked damage to erythrocytic plasma membrane. Therefore, SERS spectra of erythrocytes originate from Hb inside the intact living erythrocytes, but not from Hb_c, which may have leaked from the erythrocytes due to hemolysis.

We found that erythrocytes mixed with Ag NPs show no changes in plasma membrane fluidity in the deep hydrophobic regions (2.2 nm from membrane surfaces) in the comparison to erythrocytes mixed with NaCl solution (Fig. 4 *b*). The absence of alteration in the membrane fluidity indicates that 1), Ag NPs do not affect the lipid phase of the membrane, i.e., the order of lipid molecules and their interactions with

TABLE 1 Positions and assignments of bands in RS and SERS spectra of erythrocytes and hemoglobin

Frequency (cm^{-1})	Bond of heme molecule	Symmetry of vibration	Sensitivity of vibration	Form of Hb
1640	C_aC_m, C_aC_mH, C_aC_b	B1g, ν10	Redox and spin state of Fe, presence of ligand	HbO_2
1620–1623	(C_1C_2)vinyl			HbO_2,dHb
1608	C_aC_m, C_aC_mH, C_aC_b	B1g, ν10	Redox and spin state of Fe, presence of ligand	dHb
1588	C_aC_m, C_aC_mH	A2g	Spin state of Fe, diameter of heme ring	Usually HbO_2
1565–1566	C_bC_1, C_bC_b	B1g/A1g	Redox and spin state of Fe	HbO_2
1552	C_aC_m, C_aC_mH	A2g	Spin state of Fe, diameter of heme ring	Usually dHb
1502	C_aC_m, C_aC_b, C_aN	A1g	Redox and spin state of Fe	HbO_2
1430–1435	C_aC_m	B2g	Spin state of Fe, diameter of heme ring	Usually HbO_2
1401	C_aC_b, C_bC_1, $C_aC_bC_b$	B2g	Redox state of Fe, presence of ligand	HbO_2
1375	Pyrrol half-ring, symmetric	A1g, ν4	Redox state of Fe, presence of ligand	HbO_2
1345	$C_{2vinyl}H$			HbO_2
1305	All above	ν21	Redox and spin state of Fe, presence of ligand	HbO_2
1172	Pyrrol half-ring, asymmetric	B2g, ν30	Redox state of Fe, presence of ligand	HbO_2
1155		ν44		HbO_2
1127	$C_b - CH_3$	B1g, ν5		HbO_2
1090	$= C_{2vinyl}H$			HbO_2
1003	Phenylalanine			
974	$HC_a =$			HbO_2, dHb
827	C_mH	B1u, ν10		HbO_2, dHb
795–789		A1g, ν6		HbO_2, dHb
754	Heme breathing	B1g, ν15		HbO_2, dHb
676	C_bC_1, C_aC_b, C_bC_aN	B1g, ν7		HbO_2

Data are from the literature (2,38–40).

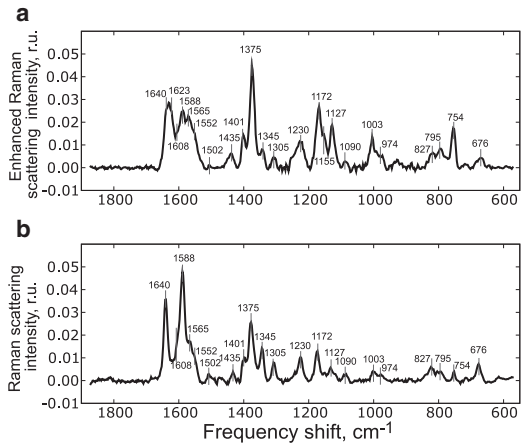

FIGURE 3 (*a*) SERS spectrum of erythrocytes mixed with Ag NP solution in a volume ratio of [Ag NP solution]:[experimental erythrocyte sample] = 2:3 and (*b*) RS spectrum of erythrocytes prepared from the same blood sample as in the SERS experiment. SERS and RS spectra are normalized to the sum of the intensities in the region of 1618–1503 cm^{-1}. Position of peaks is indicated by vertical lines.

one another and transmembrane proteins; and 2), that there is no penetration or deep intercalation of Ag NPs into the plasma membrane of erythrocytes.

Microscopical monitoring showed no change in morphology of erythrocytes mixed with Ag NPs and erythrocytes exposed only to hyperosmolar conditions (control sample 1) in the comparison with the control erythrocytes (control sample 2) (Fig. 4 *c* and Fig. 5, *a–c*). The stability of erythrocyte shape indicates that the procedure of experimental sample preparation, short-term exposure of erythrocytes to hyperosmolar conditions, and mixing with Ag NP solution do not affect plasma membrane properties, ion fluxes, and cytoskeleton. This result is in a complete agreement with data from the hemolysis test and EPR spectroscopy. Therefore, we can conclude that we found experimental conditions in which Ag NPs do not enter erythrocytes and do not affect the properties and integrity of plasma membrane. Thus, SERS with the above-specified Ag NP solution and experimental conditions can be used successfully for a noninvasive study of submembrane hemoglobin in intact living erythrocytes.

How to distinguish submembrane hemoglobin from free unbound cytosolic hemoglobin

For this purpose, we compare 1), Raman spectra from intact erythrocytes and from hemoglobin isolated from the cytoplasm of erythrocytes (Hb_{ic}); and 2), SERS spectra from erythrocytes, isolated Hb_{ic} and Hb, bound to AE1 exchanger of erythrocyte ghosts (Hb_{AE1}). Importantly, erythrocyte ghosts contain only Hb_{AE1}, and no cytosolic Hb; therefore, they represent a valuable model for studies of membrane-bound Hb (30).

RS spectra of erythrocytes and Hb_{ic} show no differences (Fig. 6). This similarity indicates that Hb_c and Hb_{ic} have similar properties, i.e., the same heme conformations, which can be explained by full Hb oxygenation evoked by experimental conditions. As we have shown that RS spectra of erythrocytes (Hb_c) and isolated Hb_{ic} show no difference, we can suppose that the SERS spectra of Hb_c in intact erythrocytes and isolated Hb_{ic} should also be similar. Therefore, we can assume that if Hb_c defines the SERS spectra of erythrocytes, we should observe similarity between SERS spectra of erythrocytes and Hb_{ic}, and a difference between SERS spectra of erythrocytes and Hb_{AE1} bound to AE1 exchanger in erythrocyte ghosts. However, the SERS spectra of erythrocytes and Hb_{ic} are different, and the SERS spectra of erythrocytes and erythrocyte ghosts show remarkable similarity (Fig. 7).

Firstly, in SERS spectra of Hb_{ic}, peak at 1640 cm^{-1} (vibration of C_aC_m, C_aC_mH, and C_aC_b heme bonds) has a well-defined shoulder at 1623 cm^{-1} (vibration of (C_1C_2)vinyl bond), whereas in the same region of the SERS spectra for erythrocytes and Hb_{AE1} of erythrocyte ghosts there are no defined peaks or shoulders at 1640 and 1622 cm^{-1}, but only one broad peak at 1630–1635 cm^{-1} (Fig. 7 *c*). Such a broad peak can be due to the increase in the relative input of the (C_1C_2)vinyl bond vibration, which results in the similar

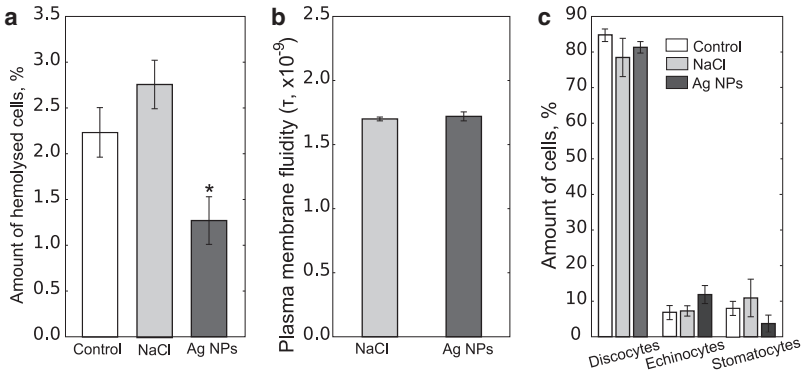

FIGURE 4 (*a*) Estimation of the hemolysis of erythrocytes in the control (*open color*) and in the samples with NaCl or Ag NP colloid solutions (*light* and *dark shading*, respectively). (*b*) Plasma membrane fluidity of erythrocytes in the samples with NaCl and Ag NP colloid solutions (*light* and *dark shading*, respectively). The value τ is a rotational correlation time of the spin-probe 16-DS with a nitroxyl radical located at 2.2 nm from the surface of the plasma membrane. The absence of change in the τ-value indicates the same membrane fluidity for erythrocytes mixed with NaCl or Ag NP colloid solutions. (*c*) Data from the morphological analysis of the effect of Ag NPs on the shape of erythrocytes. In panels *a–c*, data are shown as mean ± SE. In all cases the number of independent experiments were $n = 5$. The asterisk (*) indicates $p < 0.05$ according to the Student's *t*- test in the comparison of erythrocytes, mixed with Ag NPs, and with the control and NaCl samples.

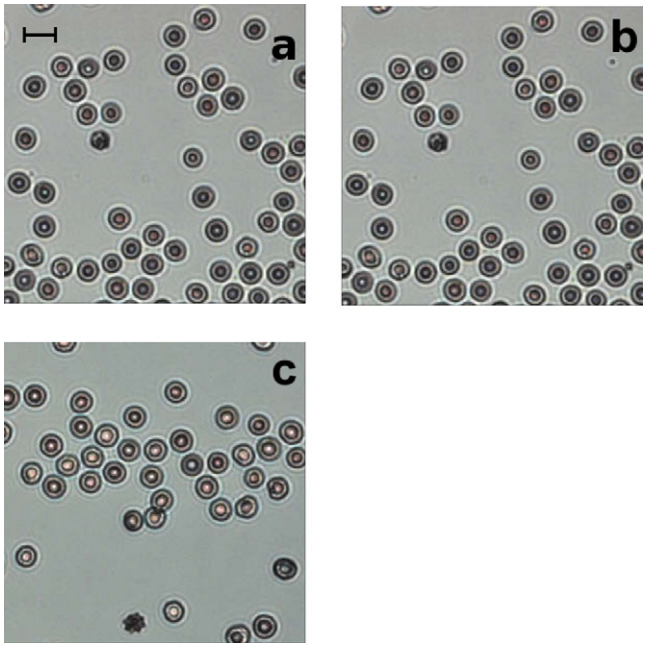

FIGURE 5 Reflected-light microphotographs of control erythrocytes (control sample 2) (*a*) and of erythrocytes mixed with NaCl (control sample 1) or Ag NP colloid solutions (*b* and *c*, respectively). Bar indicates 10 μm.

intensities of peaks at 1640 and 1623 cm^{-1} and the formation of the envelope peak with maximum at 1630–1635 cm^{-1}.

Secondly, in the SERS spectra of erythrocytes and erythrocyte ghosts, the ratio for the intensities at 1375 cm^{-1} (pyrrol half-ring symmetric vibration—C_aC_b, C_aN bonds) and 1172 cm^{-1} (pyrrol half-ring asymmetric vibration) (I_{1375}/I_{1172}) is significantly higher than for the same ratio of Hb_{ic} (Table 2, Fig. 7 *b*). This result indicates that in heme of Hb_{AE1} and Hb molecules, seen by SERS in erythrocytes, asymmetric vibrations of pyrrol half-ring are dumped and therefore the intensity of peak at 1172 cm^{-1} is lower in comparison with the peak at 1375 cm^{-1}. It is worth mentioning that the ratio I_{1375}/I_{1172} for SERS spectra of erythrocytes was practically the same (at ~1.2–1.3) for all tested volume ratios of [Ag NPs]:[experimental erythrocyte sample] = 2:8; 3:7; 2:3; 3:2 (Fig. S1). We should also note that the general view of SERS spectra of erythrocyte ghosts (number of peaks and peak positions) is completely the same, as for erythrocytes and Hb_{ic}.

In view of the obtained data, we conclude that the difference between SERS spectra of erythrocytes and Hb_{ic} and the similarity between SERS spectra of erythrocytes and Hb_{AE1} in erythrocyte ghosts is a result of 1), the significant contribution of the membrane-bound Hb_{AE1} (the same as Hb_{sm}) to SERS spectra of erythrocytes; and 2), of the difference between membrane-bound and free cytosolic Hbs.

The features of SERS spectra of erythrocytes and erythrocyte ghosts are due to vibrations of the heme bonds in membrane-bound Hb, which are different from the vibrations of heme bonds in free Hb. This finding indicates several peculiarities of Hb_{sm} conformation.

Firstly, Hb_{sm} undergoes conformational changes due to the interaction with an AE1 exchanger (16,27) and, hence, differs from the conformation of free Hb_{ic}. Due to this interaction, the heme molecule of Hb_{sm} is distorted and changes its conformation. This results in the obstruction of the vibration of some heme bonds, namely, asymmetric vibrations of the pyrrol half-ring, observed from the decrease in the intensity of the peak at 1172 cm^{-1}, in comparison with the peak at 1375 cm^{-1} (symmetric vibrations of the pyrrol half-ring). Hb_c or Hb_{ic} do not interact specifically with membrane; therefore, there are no geometrical restrictions such as for Hb_{sm}. The heme molecule of Hb_{ic}/Hb_c is more relaxed and intensities of symmetric and asymmetric pyrrol half-ring vibrations are similar. The same explanation can be applied to the difference in group vibration of the C_aC_m, C_aC_mH, and C_aC_b bonds and the (C_1C_2)vinyl bond in Hb_{sm} and Hb_{ic}. The vinyl residue can rotate around the pyrrol C_b atom, and we can suggest that the position of the vinyl relative to the pyrrol ring can be different in the heme of membrane-bound Hb and free Hb_{ic}.

Secondly, because of Hb_{sm} interaction with the AE1 exchanger, heme molecules in Hb_{sm} could be specifically oriented toward plasma membrane and therefore toward Ag NPs. It is more likely that there is no specific orientation of Hb_{ic} molecules and their heme bonds toward Ag NPs or, at least, their orientation is different in the comparison to Hb_{sm}. Thus, due to the specific orientation of Hb_{sm} heme toward Ag NPs, its symmetry can be changed and vibrational modes can be presented differently in the comparison with the heme of Hb_{ic}. This can explain the change in the relative input of the symmetrical and asymmetrical pyrrol half-ring vibrations in the heme of Hb_{sm}/Hb_{AE1} of erythrocytes and erythrocyte ghosts in comparison with the similar input of the same vibrations in Hb_{ic}. This suggestion is based on evidence that intensities and position of peaks in SERS spectra of small molecules depend on the orientation of the

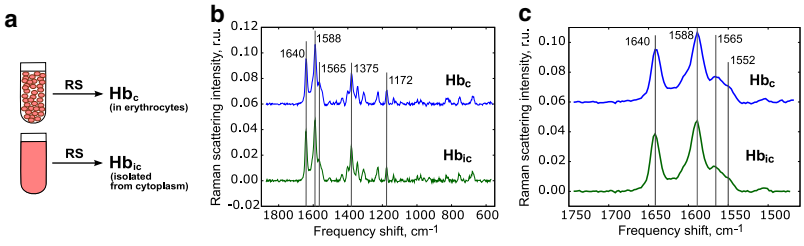

FIGURE 6 (*a*) A sample with high concentration of erythrocytes (*upper tube*) was used to obtain Raman spectra of cytosolic Hb inside living erythrocytes (Hb_c) (*b* and *c*, *upper spectra*). A sample with a high concentration of Hb released from the cytoplasm of erythrocytes (*a*, *lower tube*) was used to obtain Raman spectra of isolated cytosolic Hb (Hb_{ic}) (*b* and *c*, *lower spectra*). (*b*) A comparison of Raman spectra of Hb_c and Hb_{ic} reveals no differences in their structure and peak intensities. (*c*) An enlargement of the high frequency regions of spectra shown in panel *b*.

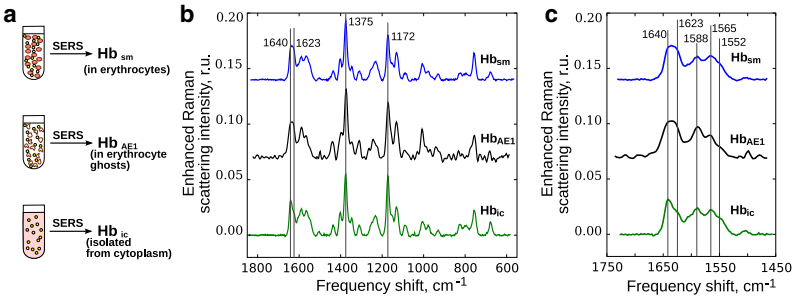

FIGURE 7 (*a*) A sample with a low concentration of erythrocytes mixed with Ag NPs (*upper tube*) was used to obtain SERS spectra of submembrane Hb inside living erythrocytes (Hb_{sm}) (*b* and *c*, *upper spectra*). A sample with a low concentration of erythrocyte ghosts (*a*, *middle tube*) was used to obtain SERS spectra of the membrane-bound Hb_{AE1} (*b* and *c*, *middle spectra*). A sample with a low concentration of Hb, released from the cytoplasm of erythrocytes (*a*, *lower tube*), was used to obtain SERS spectra of Hb_{ic} (*b* and *c*, lower spectra). (*b*) Comparison of the SERS spectra of Hb_{sm}, Hb_{AE1}, and Hb_{ic} shows that the ratio for the intensities with maxima at 1375 cm^{-1} and 1172 cm^{-1} is similar for Hb_{sm} and Hb_{AE1} and different in the comparison of Hb_{sm} and Hb_{AE1} with Hb_{ic}. (*c*) The enlargements of the high-frequency regions of the SERS spectra for Hb_{sm}, Hb_{AE1}, and Hb_{ic} show two peaks with maxima at 1640 cm^{-1} and 1623 cm^{-1} for Hb_{ic} and one peak with maximum at 1630–1635 cm^{-1} for Hb_{sm} and Hb_{AE1}.

studied bonds toward NPs (41–43). Therefore, it is natural to conclude that the orientation of large biomolecules toward NPs also affects their SERS signal.

Because we concluded from RS and SERS experiments with erythrocytes and isolated Hb, that 1), conformations of Hb_c and Hb_{ic} are similar, and 2), conformations and/or orientation of Hb_{sm} and Hb_{ic} are different, we assume that conformations of Hb_c and Hb_{sm} are also different or/and that there is a specific orientation of Hb_{sm} toward Ag NPs and plasma membrane.

Both assumptions are of significant interest. Differences in conformations of Hb_c and Hb_{sm} could imply different affinities to O_2. In particular, symmetric and asymmetric vibrations of pyrrol half-ring are sensitive to the redox state of the Fe atom and the presence of ligand, e.g., O_2 (38–40) and the relative intensity of 1375 cm^{-1} peak was already proposed for the estimation of Hb oxygenation (44). The possible distortion of heme resulting in the observed change in the vibrations of pyrrol half-ring can affect Hb ability to bind O_2. Moreover, regulation of O_2-binding properties of Hb_c and Hb_{sm} can also be different. By means of AS it has already been shown that Hb, bound to the cytosolic part of AE1 exchanger, is less sensitive to 2,3-diphosphoglycerate and inositol hexaphosphate than free Hb (27,45). We propose to use SERS to explore Hb_{sm} properties in intact living erythrocytes and to compare Hb_{sm} with Hb_c.

CONCLUSION

This article illustrates the application of SERS to studies of submembrane Hb in living erythrocytes.

TABLE 2 Intensity ratios I_{1375}/I_{1172} for SERS spectra of intact erythrocytes, erythrocyte ghosts with membrane-bound Hb, and isolated Hb from erythrocyte cytoplasm

	Intact erythrocytes	Erythrocyte ghosts	Hb_{ic} isolated from erythrocyte cytoplasm
I_{1375}/I_{1172}, mean value	1.332*	1.245*	1.005
Mean ± SE	0.059	0.039	0.007
n	7	7	7

*$p < 0.05$, according to the Student's *t*- test in the comparison with Hb_{ic}.

Despite numerous data on the application of SERS in organic chemistry and biochemistry, there is still a lack of SERS experiments performed on living cells. There is, furthermore, no analysis of the possible negative effects of nanoparticles on studied cells. Here we report optimal conditions for SERS studies of living nonmodified erythrocytes using Ag NPs. We have used three independent techniques to demonstrate that the proposed conditions of SERS experiments and Ag NPs themselves do not affect the properties of erythrocytes.

To our knowledge, we are the first to demonstrate that SERS spectra of erythrocytes differ from SERS spectra of free isolated cytosolic Hb, but are similar to SERS spectra of the membrane-bound Hb in erythrocyte ghosts. We concluded that SERS signal of erythrocytes comes from Hb_{sm} associated with cytosolic domain of AE1 exchanger. Our data indicate that conformations of cytosolic and submembrane Hbs in living erythrocytes are different, which can cause nonsimilarity in the regulation of their O_2-binding properties. As interaction of Hb with membrane lipids seems to be insignificant under nonpathological conditions (19), we expect no contribution from the lipid-bound Hb. However, we could not completely reject the possible minor contribution of Hb_c, located nearby the membrane, to the SERS spectrum of erythrocytes.

Further application of SERS to living erythrocytes will shed light on the interaction of Hb with plasma membrane and on the influence of regulatory molecules, submembrane processes, and drugs on hemoglobin properties. Thus, the combination of SERS and RS can help in the study of the effects of stimuli on two hemoglobin populations (Hb_c and Hb_{sm}) and to elucidate whether submembrane hemoglobin molecules play a significant role in the saturation of the whole erythrocyte with O_2.

SUPPORTING MATERIAL

Three figures are available at http://www.biophysj.org/biophysj/supplemental/S0006-3495(09)01511-2.

We are grateful for the useful discussions with and support of Prof. Erik Mosekilde, and to Dr. Charlotte Mehlin Sørensen for the rat blood provided.

Support for this work came from the Det Frie Forskningsraad for Natur og Univers (to N.A.B. and O.V.S.), and the Danish National Research Foundation (support to S.A. for QuP research). This work was partly supported by the European Commission (NoE BioSim, Contract No. LSHB-CT-2004-005137), the Russian Foundation of Basic Research (grant Nos. 070400621, 080400531, 090400646, and 090312221), and the Federal Purpose-Oriented Program of the Russian Federation for 2008–2010 (lot No. 5, 2008-3-3.1-049).

REFERENCES

1. Friedman, J. M. 1985. Structure, dynamics, and reactivity in hemoglobin. *Science*. 228:1273–1280.
2. Wood, B. R., P. Caspers, G. J. Puppels, S. Pandiancherri, and D. McNaughton. 2007. Resonance Raman spectroscopy of red blood cells using near-infrared laser excitation. *Anal. Bioanal. Chem.* 387: 1691–1703.
3. Fu, Y., H. Wang, T. B. Huff, H.-W. Wang, J. X. Cheng, et al. 2008. Ex vivo and in vivo imaging of myelin fibers in mouse brain by coherent anti-Stokes Raman scattering microscopy. *Opt. Express.* 16:19396–19409.
4. Fleishmann, M., P. J. Hendra, and A. J. McAuillan. 1974. Raman spectra of pyridine adsorbed at a silver electrode. *Chem. Phys. Lett.* 26:163–166.
5. Moskovits, M. 1985. Surface-enhanced spectroscopy. *Rev. Mod. Phys.* 57:783–827.
6. Wang, Z., S. Pan, T. D. Krauss, H. Du, and L. J. Rothberg. 2003. The structural basis for giant enhancement enabling single-molecule Raman scattering. *Proc. Natl. Acad. Sci. USA.* 100:8638–8643.
7. Wokaun, A., H. D. Lutz, A. P. King, U. P. Wild, and R. R. Ernst. 1983. Energy transfer in surface enhanced luminescence. *J. Chem. Phys.* 79:509–514.
8. Ray, K., H. Szmacinski, J. Enderlein, and J. R. Lakowicz. 2007. Distance dependence of surface plasmon-coupled emission observed using Langmuir-Blodgett films. *Appl. Phys. Lett.* 90:251116.
9. Lakowicz, J. R., K. Ray, M. Chowdhury, H. Szmacinski, Y. Fu, et al. 2008. Plasmon-controlled fluorescence: a new paradigm in fluorescence spectroscopy. *Analyst (Lond.).* 133:1308–1346.
10. Delfino, I., A. R. Bizzarri, and S. Cannistraro. 2005. Single-molecule detection of yeast cytochrome *c* by surface-enhanced Raman spectroscopy. *Biophys. Chem.* 113:41–51.
11. Kneipp, J., H. Kneipp, and K. Kneipp. 2006. Two-photon vibrational spectroscopy for biosciences based on surface-enhanced hyper-Raman scattering. *Proc. Natl. Acad. Sci. USA.* 103:17149–17153.
12. Abdali, S., C. Johannessen, J. Nygaard, and T. Norbygaard. 2007. Resonance surface enhanced Raman optical activity of myoglobin as a result of optimized resonance surface enhanced Raman scattering conditions. *J. Phys. Condens. Matter.* 103:285205-1–285205-8.
13. Xie, W., L. Wang, Y. Zhang, L. Su, A. Shen, et al. 2009. Nuclear targeted nanoprobe for single living cell detection by surface-enhanced Raman scattering. *Bioconjug. Chem.* 20:768–773.
14. Bernhardt, I. and C. Ellory, editors. 2003. Red Cell Membrane Transport in Health and Disease. Springer, Heidelberg.
15. Shaklai, N., J. Yguerabide, and H. M. Ranney. 1977. Interaction of hemoglobin with red blood cell membranes as shown by a fluorescent chromophore. *Biochemistry.* 16:5585–5592.
16. Walder, J. A., R. Chatterjee, T. L. Steck, P. S. Low, G. F. Musso, et al. 1984. The interaction of hemoglobin with the cytoplasmic domain of band 3 of the human erythrocyte membrane. *J. Biol. Chem.* 259:10238–10246.
17. Chen, Q., T. C. Balazs, R. L. Nagel, and R. E. Hirsch. 2006. Human and mouse hemoglobin association with the transgenic mouse erythrocyte membrane. *FEBS Lett.* 580:4485–4490.
18. Shaklai, N., J. Yguerabide, and H. M. Ranney. 1977. Classification and localization of hemoglobin binding sites on the red blood cell membrane. *Biochemistry.* 16:5593–5597.
19. Shaklai, N., and H. R. Ranney. 1978. Interaction of hemoglobin with membrane lipids: a source of pathological phenomena. *Isr. J. Med. Sci.* 14:1152–1156.
20. Shaklai, N., H. M. Ranney, and V. Sharma. 1981. Interactions of hemoglobin S with the red cell membrane. *Prog. Clin. Biol. Res.* 51:1–16.
21. Byers, T. J., and D. Branton. 1985. Visualization of the protein associations in the erythrocyte membrane skeleton. *Proc. Natl. Acad. Sci. USA.* 82:6153–6157.
22. McGough, A. M., and R. Josephs. 1990. On the structure of erythrocyte spectrin in partially expanded membrane skeletons. *Proc. Natl. Acad. Sci. USA.* 87:5208–5212.
23. Liu, F., J. Burgess, H. Mizukami, and A. Ostafin. 2003. Sample preparation and imaging of erythrocyte cytoskeleton with the atomic force microscopy. *Cell Biochem. Biophys.* 38:251–270.
24. Tyler, J. M., W. R. Hargreaves, and D. Branton. 1979. Purification of two spectrin-binding proteins: biochemical and electron microscopic evidence for site-specific reassociation between spectrin and bands 2.1 and 4.1. *Proc. Natl. Acad. Sci. USA.* 76:5192–5196.
25. Zhang, D., A. Kiyatkin, J. T. Bolin, and P. S. Low. 2000. Crystallographic structure and functional interpretation of the cytoplasmic domain of erythrocyte membrane band 3. *Blood.* 96:2925–2933.
26. van Kampen, E. J., and W. G. Zijlstra. 1983. Spectrophotometry of hemoglobin and hemoglobin derivatives. *Adv. Clin. Chem.* 23:199–257.
27. Zhang, Y., L. R. Manning, J. Falcones, O. Platt, and V. Manning. 2003. Human erythrocyte membrane band 3 protein influences hemoglobin cooperativity. Possible effect on oxygen transport. *J. Biol. Chem.* 278:39565–39571.
28. Barker, S. J., and J. J. Badal. 2008. The measurement of dyshemoglobins and total hemoglobin by pulse oximetry. *Curr. Opin. Anaesthesiol.* 21:805–810.
29. Leopold, N., and B. Lendl. 2003. A new method for fast preparation of highly surface-enhanced Raman scattering (SERS) active silver colloids at room temperature by reduction of silver nitrate with hydroxylamine hydrochloride. *J. Phys. Chem. B.* 107:5723–5727.
30. Salhany, J. M., K. A. Cordes, and R. L. Sloan. 2007. Characterization of the pH dependence of hemoglobin binding to band 3. Evidence for a pH-dependent conformational changes within the hemoglobin-band 3 complex. *Biochim. Biophys. Acta.* 1371:107–113.
31. Schreier-Muccillo, S., and O. Marsh. 1976. Monitoring the permeability profile of lipid membranes with spin probes. *Arch. Biochem. Biophys.* 172:1–11.
32. Luneva, O. G., N. A. Brazhe, N. V. Maksimova, O. V. Rodnenkov, E. Y. Parshina, et al. 2007. Ion transport, membrane fluidity and hemoglobin conformation in erythrocyte from patients with cardiovascular diseases: role of augmented plasma cholesterol. *Pathophysiology.* 14:41–46.
33. Gedde, M. M., E. Yang, and W. H. Huestis. 1999. Resolution of the paradox of red cell shape changes in low and high pH. *Biochim. Biophys. Acta.* 1417:246–253.
34. Gerald, L. H. W., M. Wortis, and R. Mukhopadhyay. 2002. Stomatocyte-discocyte-echinocyte sequence of the human red blood cell: evidence for the bilayer-couple hypothesis from membrane mechanics. *Proc. Natl. Acad. Sci. USA.* 99:16766–16769.
35. Deuticke, B. 2003. Membrane lipids and proteins as a basis of red cell shape and its alterations. *In* Red Cell Membrane Transport in Health and Disease. I. Bernhardt and C. Ellory, editors. Springer, Heidelberg.
36. Owen, J. S., D. J. Brown, D. S. Harry, N. McIntyre, G. H. Beaven, et al. 1985. Erythrocyte echinocytosis in liver disease. Role of abnormal plasma high density lipoproteins. *J. Clin. Invest.* 76:2275–2285.
37. Feinberg, T. E., C. D. Cianci, J. C. Pehta, C. M. Redman, T. Huima, et al. 1991. Diagnostic tests for choreoacanthocytosis. *Neurology.* 41:1000–1006.
38. Stein, P., I. M. Burke, and T. G. Spiro. 1975. Structural interpretation of heme protein resonance Raman frequencies. Preliminary normal coordinate analysis results. *J. Am. Chem. Soc.* 97:2304–2305.
39. Kitagawa, T., Y. Kyogoku, and T. Iizuka. 1976. Nature of the iron ligand bond in ferrous low spin hemoproteins studied by resonance Raman scattering. *J. Am. Chem. Soc.* 98:5169–5173.

40. Choi, S., T. G. Spiro, K. C. Langry, K. M. Smith, D. L. Budd, et al. 1982. Structural correlations and vinyl influences in resonance Raman spectra of protoheme complexes and proteins. *J. Am. Chem. Soc.* 104:4345–4351.

41. Moskovits, M., and J. S. Suh. 1984. Surface selection rules for surface-enhanced Raman spectroscopy: calculations and application to the surface-enhanced Raman spectrum of phthalazine on silver. *J. Chem. Phys.* 88:5526–5530.

42. Brolo, A. G., Z. Jiang, and D. E. Irish. 2003. The orientation of 2,2′-bipyridine adsorbed at a SERS-active Au^{111} electrode surface. *J. Electroanal. Chem.* 547:163–172.

43. Janesko, B. G., and G. E. Scuseria. 2006. Surface enhanced Raman optical activity of molecules on orientationally averaged substrates: theory of electromagnetic effects. *J. Chem. Phys.* 125:124704.

44. Filho, I. P. T., J. Terner, R. N. Pittman, E. Proffitt, and K. R. Ward. 2008. Measurement of hemoglobin oxygen saturation using Raman microspectroscopy and 532-nm excitation. *J. Appl. Physiol.* 104: 1809–1817.

45. Tsuneshige, A., K. Imai, and I. Tyuma. 1987. The binding of hemoglobin to red cell membrane lowers its oxygen affinity. *J. Biol. Chem.* 101:695–704.